Precision measurements of the ground-state hyperfine splitting of ^{85}Rb using an atomic fountain clock

Qian Wang,[1,2] Ning Zhang,[1,2] Wei Guang,[3] Shougang Zhang,[3] Wenli Wang,[1] Rong Wei,[1,*] and Yuzhu Wang[1]

[1]*Key Laboratory for Quantum Optics, Shanghai Institute of Optics and Fine Mechanics, Chinese Academy of Sciences, Shanghai 201800, China*

[2]*Center of Materials Science and Optoelectronics Engineering, University of Chinese Academy of Sciences, Beijing 100049, China*

[3]*National Time Service Center, Chinese Academy of Sciences, Xi'an 710600, China*

(Received 28 April 2019; published 19 August 2019; corrected 4 September 2019)

The ground state hyperfine splitting of ^{85}Rb was measured precisely using a rubidium-85 atomic fountain clock. About 5×10^5 atoms were detected at the temperature of 4 μK, and a Ramsey fringe was obtained with FWHM of 0.95 Hz. We present a measurement of the ^{85}Rb ground state hyperfine splitting with a 5×10^{-14} uncertainty. The measured ^{85}Rb ground-state hyperfine splitting was $\upsilon = 3.035\,732\,444\,821\,8(2)$ GHz. This measurement is more precise than previously reported values by 4 orders of magnitude, and differs from the previously reported value by 5.8218 Hz.

DOI: 10.1103/PhysRevA.100.022510

I. INTRODUCTION

In recent years, atomic fountain clocks (AFCs) have been improved greatly and widely applied in many atomic physics fields such as time measurement. As a central part of primary frequency standards, AFCs have increased the precision of the SI second [1] to the uncertainty of 10^{-16} [2]. The clock frequency of ^{87}Rb is used as a secondary standard of the second [3] because of the excellent performance of ^{87}Rb AFCs. AFCs using the two media (^{133}Cs and ^{87}Rb) have been running continuously in time labs worldwide [4] with long-term frequency stability of 10^{-16}–10^{-17} and frequency uncertainty of 10^{-16}.

^{85}Rb, the other natural rubidium atomic isotope, plays a key role in many investigations, such as Bose-Einstein condensates [5,6], Feshbach resonance [7,8], degenerate quantum gas [9], atomic clocks [10], and atomic interferometers [11]. Atomic fountain devices of ^{85}Rb have been built for interferometer experiments [12], but, to our knowledge, no ^{85}Rb AFC has ever been reported. The low clock frequency of ^{85}Rb (3.0 GHz) means that such a clock will have worse short-term stability ($\sigma \propto 1/\upsilon$) than ^{133}Cs (9.2 GHz) and ^{87}Rb (6.8 GHz) if all other parameters are the same. Although a ^{85}Rb AFC has its own disadvantages as a practical frequency standard, it does have advantages as follows. First, the use of this isotope will increase the measurement accuracy of the clock frequency of ^{85}Rb by 6–7 orders of magnitude over the uncertainty of 2×10^{-9} that was published in the 1970s [13]. Second, by comparing the clock frequencies of ^{85}Rb and ^{87}Rb, one can test the temporal variation of fundamental constant α [14–16]. Third, some characteristics of ^{85}Rb make many interesting research efforts on ^{85}Rb AFCs feasible. For example, the signs of the collisional shift coefficients of the two clock states are opposite, which suggests that the collisional shift can be eliminated by adjusting the atomic population ratio of the two clock states in the fountain [17,18]. In this paper, we report the measurement of the ground-state hyperfine splitting of ^{85}Rb and evaluate the frequency uncertainty using a ^{85}Rb AFC.

II. DEVICE AND OPERATION

The ^{85}Rb AFC includes physical, optical, microwave, and data processing components. The structure of the ^{85}Rb fountain setup is shown in Fig. 1. The apparatus consists of a magneto-optical trap (MOT) region, a two-level detection region, and a Ramsey interaction region. The vacuum cavity is made of aluminum and is kept at a vacuum of 2×10^{-7} Pa with a 40 L/s ion pump and eight getters. A TE_{011} copper cylindrical cavity with height and diameter of 130.2 mm has a quality factor $Q \approx 27\,000$ and is installed at the bottom of the Ramsey interaction region, and the cavity has four symmetrical coupled microwave ports. Four layers of permalloy magnetic shields, a solenoid coil, and several compensation coils provide an uniform magnetic field that fluctuates less than 1 nT. The optical system layout is shown in Fig. 2. The laser source is shared with the ^{87}Rb AFC and is split into cooling, repumping, and probing light. Cooling light is amplified by a homemade injection-locked laser amplifier. Its frequency is shifted with acousto-optic modulators (AOMs). The repumping light is resonated with $|F = 2\rangle \rightarrow |F = 3'\rangle$, and is created by a fiber electro-optical modulator (FEOM). The microwave field is generated from a signal generator (E8257C) that uses a 5 MHz output signal of a H maser (VCH-1003A) as a reference signal, which is linked to international atomic time (TAI) by GPS PPP (Global Positioning System precise point positioning) [19]. The analog and digital signals are controlled and processed by a computer.

The operation timing of the ^{85}Rb AFC is diagramed in Fig. 3. About 10^6 atoms are first trapped in a MOT, and

*weirong@siom.ac.cn

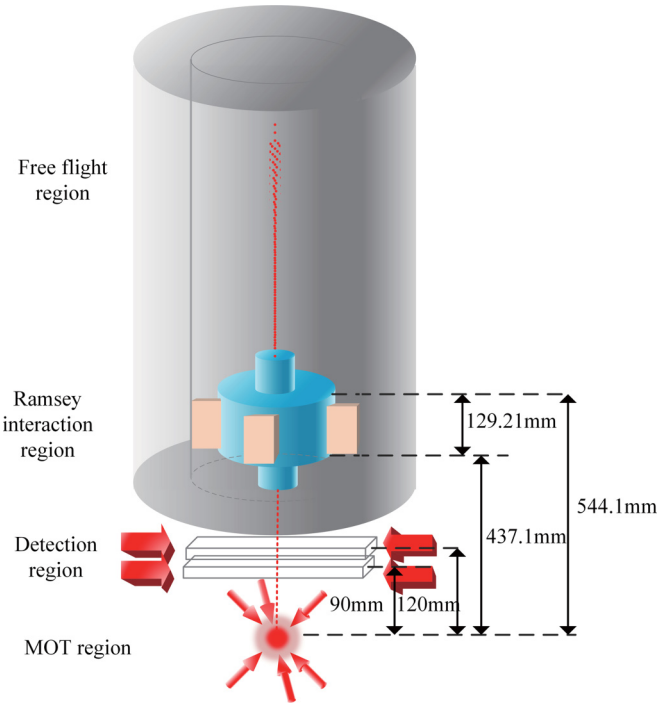

FIG. 1. Structure of the ^{85}Rb fountain setup. The typical independent microwave state-selection cavity is replaced by a microwave antenna that is installed on one side of the MOT cavity polyhedron structure. From the bottom to the top are the MOT region, the two-level detection region, the Ramsey interactions region, and the free flight region, respectively.

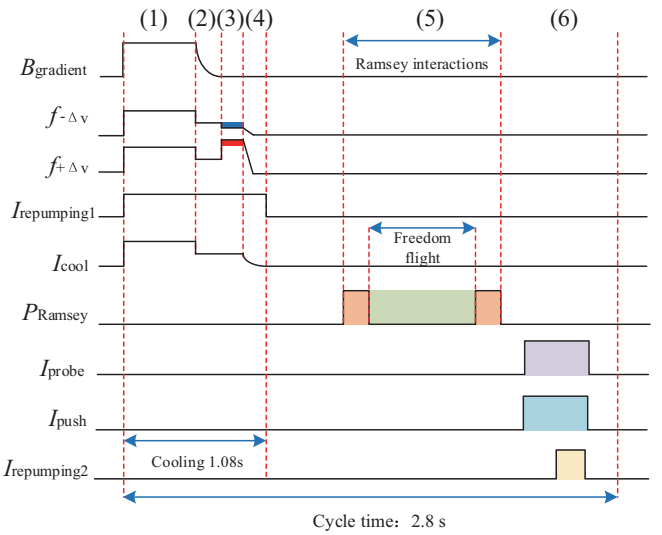

FIG. 3. Operation timing of the ^{85}Rb fountain. (1) MOT. (2) Molasses. (3) Launch. (4) Post-cooled. (5) Ramsey interactions. (6) Detection. State selection is generally set between steps (4) and (5). Atomic cooling and trapping time: 1.08 s; execute cycle time: 2.8 s.

cooled by optical molasses, then launched in (1,1,1) geometry by moving optical molasses with an initial velocity of 3.97 m/s (corresponding to a launch height of 805 mm) in 0.8 ms and post-cooled to a temperature of about 4 μK. During the ballistic flight, the atoms pass through the Ramsey cavity twice. A $\pi/2$ microwave pulse fed into the cavity from one of the four ports induces the ground-state transition of $|F = 3, m_F = 0\rangle \rightarrow |F = 2, m_F = 0\rangle$. Finally the atoms are measured using the time-of-flight (TOF) method as they fall through the two-level detection region, shown in Fig. 4(a). From the TOF signal, we obtain the atom numbers of the two ground hyperfine states, which are $N_{F=2} = 7 \times 10^4$ and $N_{F=3} = 5 \times 10^5$, respectively, and the atomic temperature is 4 μK. The transition probability is calculated with $P = N_{F=2}/(N_{F=2} + N_{F=3})$. The typical Ramsey interference fringe is shown in Fig. 4(b), in which each data point is an average of 12 repetitions. The full width at half maximum (FWHM)

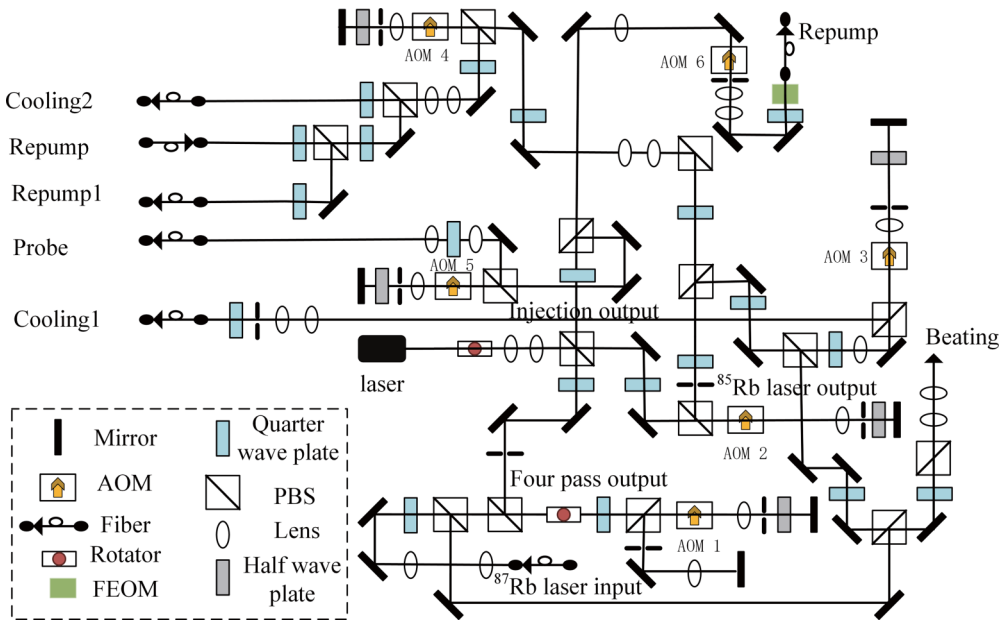

FIG. 2. Simplified scheme of the laser optical system for the ^{85}Rb AFC.

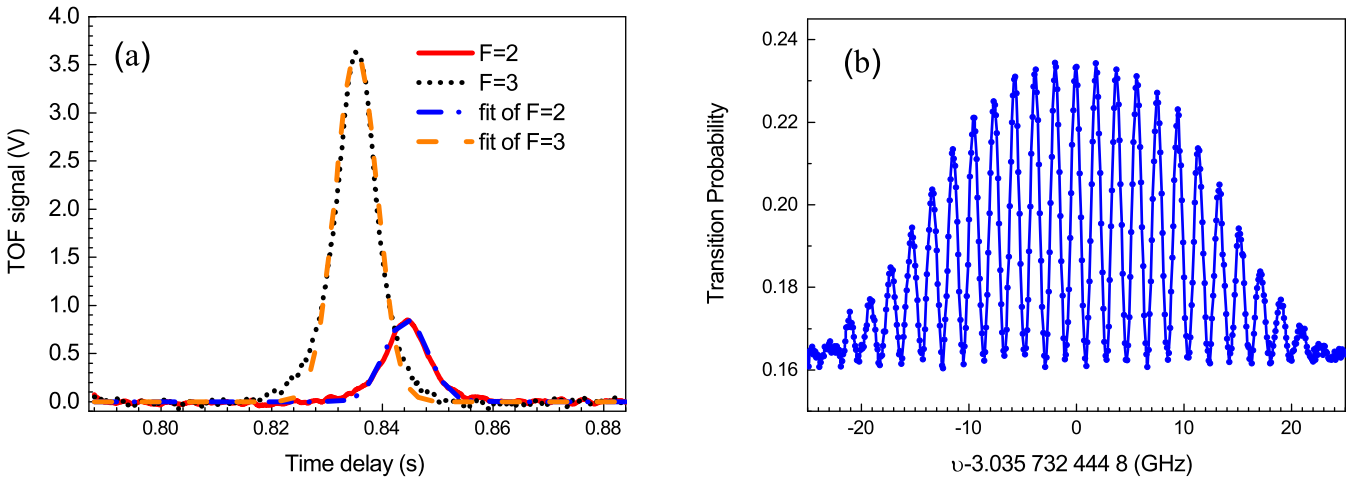

FIG. 4. (a) Falling TOF signal. The solid red, dotted black, dash-dotted blue, and dashed orange lines represent the TOF signals of $F = 2$, $F = 3$, a Gaussian fit of $F = 2$, and a Gaussian fit of $F = 3$, respectively. The atomic numbers of $F = 2$ ($N_{F=2}$) and $F = 3$ ($N_{F=3}$) are 7×10^4 and 5×10^5, respectively. (b) Ramsey interference fringe at the height of 805 mm. The transition probability $P = N_{F=2}/(N_{F=2} + N_{F=3})$, averaged over 12 repetitions, is plotted as a function of microwave frequency detuning with frequency-scanning intervals of 0.1 Hz. The FWHM of the central Ramsey fringe is 0.95 Hz and the contrast is about $0.08/0.2 = 0.4$. The Ramsey fringe is shifted by +5.8 Hz from the previously published value of 3.035 732 439 0(60) GHz.

of the central fringe is $\Delta\upsilon = 0.95$ Hz. Figure 4(b) also shows that the clock frequency of ^{85}Rb is $\upsilon_0 = 3.035\,732\,444\,8$ GHz, which is about +5.8 Hz different from the previously published value [13]. More precise measurements of the clock frequency are achieved in the comparative experiments.

III. PRELIMINARY EVALUATION

The frequency stability of the AFC was measured in an open-loop comparative experiment, in which the device records only the error signal and does not feed back to the reference (H maser). The interrogation error is obtained with square-wave modulation, and comes from the difference in the probability of two successive measurements at the frequencies of $\upsilon_0 - \Delta\upsilon$ and $\upsilon_0 + \Delta\upsilon$. The central frequency is set to 3.035 732 444 824 GHz. The frequency stability of the comparative data, expressed in terms of Allan deviation, is $1.4 \times 10^{-11}\tau^{-1/2}$, and reaches 4×10^{-14} at the integral time of 7×10^4 s, as shown in Fig. 5. The fractional frequency bias of the H maser that is compared against the TAI signal is 5.42×10^{-13} with a frequency uncertainty of 7×10^{-15} at integral time of 10^4 s. The short-term frequency stability of this device is worse than that of other AFCs, because its atom numbers are smaller than those of other AFCs due to the low laser power and the relatively large optical noise. In future work, we plan to use a better laser source and make other improvements such as installing a low-noise microwave synthesizer and adding a state-selection process. These improvements are expected to improve the short-term frequency stability to better than $5 \times 10^{-13}\tau^{-1/2}$.

The clock frequency of ^{85}Rb was measured with a precision of 10^{-14}, and this precision was limited by the frequency stability of the clock. At this level, only a few physical effects contribute to the frequency error and uncertainty of the AFC. Below, we evaluate the contributions of second-order Zeeman shift, blackbody radiation shift, collisional shift, and the microwave-related frequency shift.

The second-order Zeeman effect is a major effect on the $|3, 0\rangle \rightarrow |2, 0\rangle$ transition of the ^{85}Rb ground state. The magnetic field sensitive Ramsey transition $|3, -1\rangle \rightarrow |2, -1\rangle$ was used to evaluate the average magnetic intensity [20–22]. The magnetic field sensitive Ramsey interference fringe and C-field mapping are shown in Figs. 6(a) and 6(b), respectively. The fractional frequency shift due to the second-order Zeeman effect can be evaluated by the Breit-Rabi formula [23]:

$$\frac{\Delta\upsilon_{|3,0\rangle\rightarrow|2,0\rangle}}{\upsilon_0} = \frac{k_2\left(\frac{\Delta\upsilon_{|3,-1\rangle\rightarrow|2,-1\rangle}}{k_1}\right)^2}{\upsilon_0} = 3.51 \times 10^{-13}, \quad (1)$$

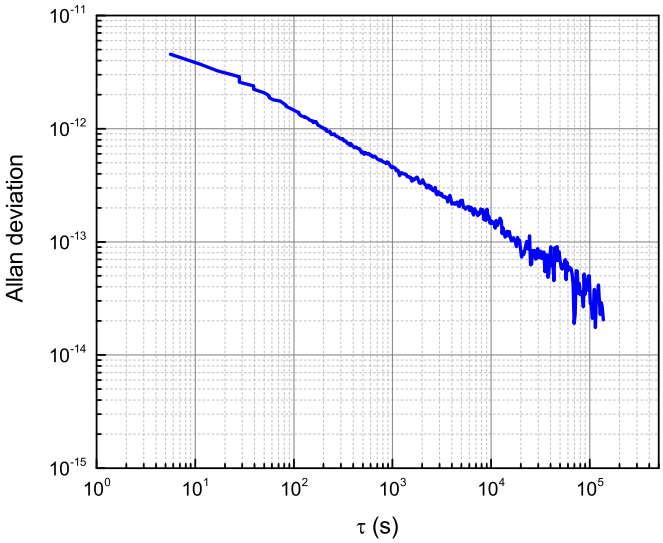

FIG. 5. Fractional frequency stability of the ^{85}Rb AFC as measured in an open-loop experiment run for more than two days. The short-term fractional frequency stability is about $1.4 \times 10^{-11}\tau^{-1/2}$. At 7×10^4 s, the frequency stability reaches 4×10^{-14}.

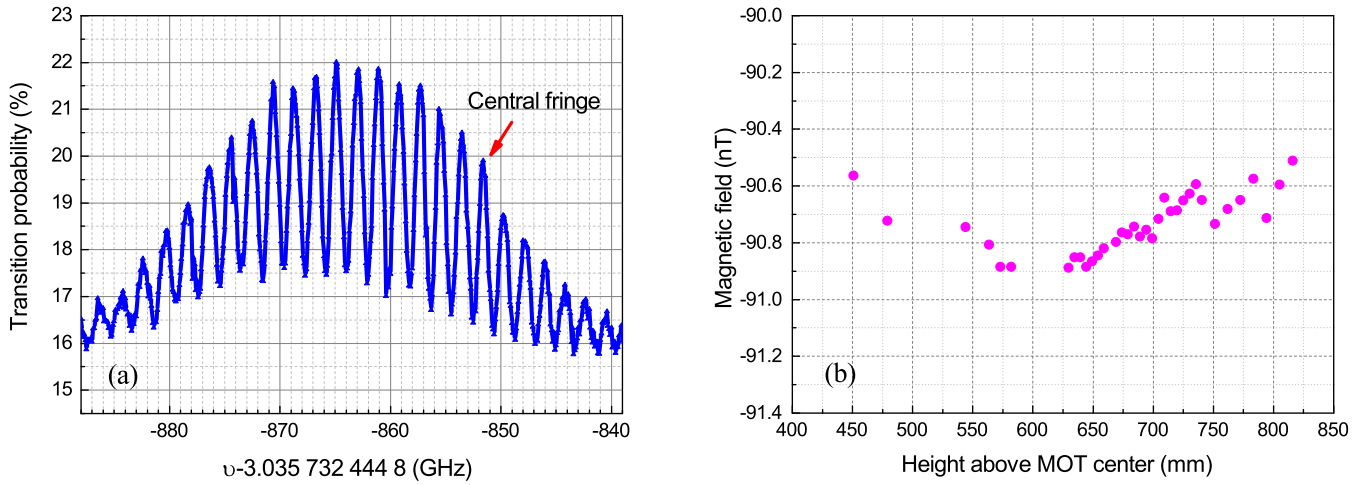

FIG. 6. (a) Ramsey fringes for the $|3,-1\rangle \rightarrow |2,-1\rangle$ transition at the launch height of 805 mm. The red arrow marks the central fringe. The distortion of the fringe is attributed to inhomogeneous broadening of the magnetic field. (b) C-field mapping above the center of the MOT chamber. The magnetic field fluctuates within 0.4 nT.

where $k_1 = 0.47$ MHz/G and $k_2 = 1293.98$ Hz/G^2 are the first- and second-order Zeeman frequency shift coefficients, respectively, and $\Delta\upsilon_{|3,0\rangle\rightarrow|2,0\rangle} = -851.5$ Hz at the height of 805 mm. The fluctuation of magnetic intensity and deviation of the magnetic field sensitive Ramsey central fringe are less than 0.4 nT and 1 Hz, respectively, and these introduce frequency uncertainty of 10^{-15}.

During the ballistic flight, the atoms experience an ac Stark shift caused by blackbody radiation. This effect is related to the temperature of the Ramsey interaction region, and the resulting fractional frequency shift is expressed as follows:

$$\frac{\Delta\upsilon}{\upsilon_0} = \beta\left(\frac{T(K)}{T_0}\right)^4\left(1+\varepsilon\left(\frac{T(K)}{T_0}\right)^2\right), \tag{2}$$

where T_0 is usually assumed to be equal to room temperature (300 K) and ε is a small correction resulting from frequency distribution [24,25]. The higher order term in Eq. (2) can be neglected here. $k = 0.546 \times 10^{-10}$ Hz/(V/m)^2 for ^{85}Rb [26], k and β are related through the following equation:

$$\beta = \frac{k}{\upsilon_0} \times (831.9\ \text{V/m})^2 = 1.24 \times 10^{-14}. \tag{3}$$

The vacuum cavity of the fountain is heated by an aluminum-film heater, and five PT100 thermometers are installed between the heater and the outer surface of the cavity to monitor the temperature. The temperature of the Ramsey cavity is 305 K and the fractional frequency shift is 1.32×10^{-14}. The temperature differences between the five thermometers and their fluctuations are less than ± 0.5 K. Considering that the temperatures inside and outside the cavity may differ, we magnify this error by four times to ± 2 K. This error in temperature corresponds to an uncertainty of 2×10^{-16}, which is negligible in our preliminary uncertainty evaluation.

The isotope ^{85}Rb has characteristics that are different from those of ^{133}Cs and ^{87}Rb with respect to collisional effect. For ^{85}Rb, the collisional shifts produced by the two clock states have opposite signs, so the shift can be neutralized by driving a $\pi/5$ pulse through the microwave cavity at 1 μK in the first pass [18]. However, this method will reduce the Ramsey fringe contrast by 40% [17] and deteriorate the frequency stability of the clock. For our current ^{85}Rb AFC device, the frequency stability is the main limitation of precision for evaluating of the clock frequency, so we still use $\pi/2$ microwave pulse in our simple quantitative analysis. In the absence of state-selection process, the collisional shift is evaluated as

$$\frac{\Delta\upsilon}{\upsilon_0} = \frac{\frac{1}{7}\left(\sum_{3,m_f=-3}^{3}\frac{(n\mu\lambda)_{3,m_f}}{2\pi} + \frac{1}{2}\left(\frac{(n\mu\lambda)_{2,0}}{2\pi} - \frac{(n\mu\lambda)_{3,0}}{2\pi}\right)\right)}{\upsilon_0} = -8.4 \times 10^{-15}. \tag{4}$$

In Eq. (4) the atomic density n is 3.6×10^6 cm^{-3}. The collisional frequency shifts $(n\mu\lambda)_{F,m_f}/2\pi$ of the ground hyperfine

TABLE I. Predicted collisional shifts $(n\mu\lambda)_{F,m_f}/2\pi$ in 10^{-5} Hz for ^{85}Rb at $E/k_B = 4$ μK and $n = 3.6 \times 10^6$ cm^{-3} [26].

F, m_f	2,0	3,0	3,±1	3, ±2	3, ±3
$(n\mu\lambda)_{F,m_f}/2\pi$	0.08	−1.22	−0.08	−0.32	−0.28

TABLE II. Main frequency shift and uncertainty budget of ^{85}Rb AFC.

Error source	Frequency shift ($\times 10^{-14}$)	Uncertainty ($\times 10^{-14}$)
Second-order Zeeman	35.1	0.1
Blackbody radiation	1.32	0.02
Cold collisional	−0.84	1
Microwave-related shift	0	3
Comparing with H maser (type A)	−16	4
Links to TAI	54	0.7
Total	73.58	5.1

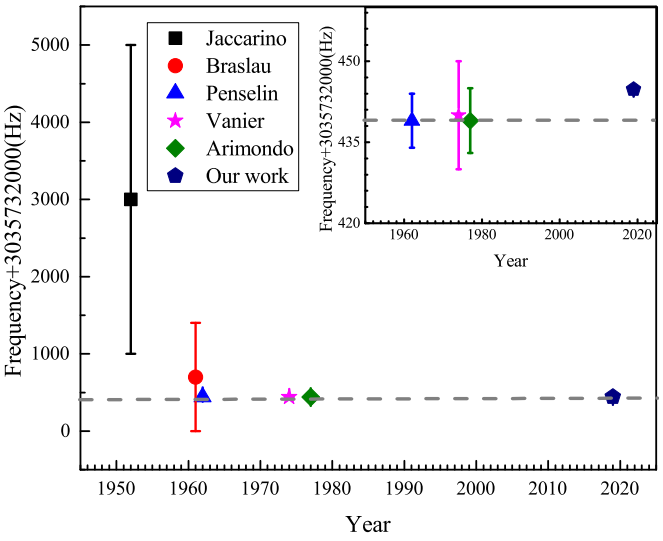

FIG. 7. The previously published values of ground-state hyperfine splitting for ^{85}Rb along with uncertainties, plotted alongside the present results. Black squares, red circles, blue triangles, pink pentagrams, olive rhombi, and navy pentagons represent the results of Jaccarino *et al.* [27], Braslau *et al.* [28], Penselin *et al.* [29], Vanier *et al.* [30], Arimondo *et al.* [13] and our work, respectively. The inset shows the results of the last four groups and the dashed gray line represents the value of published work at present.

substate of ^{85}Rb and their uncertainties are obtained from the data of Ref. [26] at the temperature of 1 μK, as shown in Table I. The resulting uncertainty in the collisional frequency shift is about 1×10^{-14}. Since the collisional frequency shift of the ^{85}Rb AFC is large and is sensitive to the temperature of the atoms, more research is necessary tp better understand this effect. This research will be important for evaluating the precision of ^{85}Rb AFCs with less uncertainty.

There are many effects related to macrowave cavity, including cavity pulling, distribution-cavity phase shift [22], and microwave leakage. We have performed many experiments to evaluate these effects, including measuring the frequency with microwaves fed to the cavity from different ports, $3\pi/2$ and $5\pi/2$ high order microwave pulses, continuous microwave feeding, and others. The differences in the calibration frequency in these experiments and normal operating conditions are less than 3×10^{-14} with uncertainty of about 6×10^{-14}, which means that the error and uncertainty of these effects are far less than 3×10^{-14}, and these can be counted directly as uncertainty. The uncertainty budget for each factor is listed in Table II. These data show that the total fractional frequency shift is 7.36×10^{-13}, which is expressed as $u = \sqrt{u_A^2 + u_B^2 + u_{\text{link}}^2}$, where the values of u_A, u_B, and u_{link} are 4×10^{-14}, 3×10^{-14}, and 7×10^{-15}, respectively. The frequency uncertainty is 5×10^{-14}. After frequency correction, ^{85}Rb ground-state hyperfine splitting is $\upsilon = 3.035\,732\,444\,821\,8(2)$ GHz. We list the values of ground-state hyperfine splitting for ^{85}Rb observed in previously published research and in our work, along with the uncertainty, as a bar plot in Fig. 7.

IV. CONCLUSIONS AND OUTLOOK

An ^{85}Rb atomic fountain clock was built and run to measure the ground-state hyperfine splitting of ^{85}Rb. From preliminary comparison and evaluation experiments, we find that the short-term frequency stability of the ^{85}Rb AFC is $1.4 \times 10^{-11}\tau^{-1/2}$ and its long-term frequency stability is better than 4×10^{-14} at 7×10^4 s. The measured clock frequency was 3.035 732 444 821 8(2) GHz. Compared with the previously published clock frequency value, the result increases precision by 4 orders of magnitude and corrects the known frequency by 5.8218 Hz.

On the other hand, the performance of ^{85}Rb AFC is worse than other AFCs, and it is mainly limited by the device's short-term frequency stability. In future work, we plan to take measures to increase the frequency stability and decrease the uncertainty. Then we can do some research on ^{85}Rb, such as measuring the clock frequency of ^{85}Rb with a precision of 10^{-16}, and testing the variation of the fine-structure constant by comparing the outputs of ^{85}Rb and ^{87}Rb AFCs.

ACKNOWLEDGMENTS

We thank Qingqing Hu for useful discussions. This work is supported by the Strategic Priority Research Program of the Chinese Academy of Sciences, Grant No. XDB21030200.

[1] R. Wynands and S. Weyers, Metrologia **42**, S64 (2005).
[2] K. Gibble, S. Lea, and K. Szymaniec, in *2012 Conference on Precision Electromagnetic Measurements (CPEM 2012), July 2012, Washington* (IEEE, Piscataway, NJ, 2012), pp. 700–701.
[3] S. Peil, J. Hanssen, T. B. Swanson, J. Taylor, and C. R. Ekstrom, J. Phys.: Conf. Ser. **723**, 012004 (2016).
[4] K. Szymaniec, S. N. Lea, K. Gibble, S. E. Park, K. Liu, and P. Głowacki, J. Phys.: Conf. Ser. **723**, 012003 (2016).
[5] S. L. Cornish, N. R. Claussen, J. L. Roberts, E. A. Cornell, and C. E. Wieman, Phys. Rev. Lett. **85**, 1795 (2000).
[6] M. H. Anderson, J. R. Ensher, M. R. Matthews, C. E. Wieman, and E. A. Cornell, Science **269**, 198 (1995).
[7] S. Inouye, M. R. Andrews, J. Stenger, H. J. Miesner, D. M. Stamper-Kurn, and W. Ketterle, Nature (London) **392**, 151 (1998).
[8] P. Courteille, R. S. Freeland, D. J. Heinzen, F. A. van Abeelen, and B. J. Verhaar, Phys. Rev. Lett. **81**, 69 (1998).
[9] G. Roati, F. Riboli, G. Modugno, and M. Inguscio, Phys. Rev. Lett. **89**, 150403 (2002).
[10] Y. Ovchinnikov and G. Marra, Metrologia **48**, 87 (2011).
[11] A. Peters, K. Y. Chung, and S. Chu, Nature (London) **400**, 849 (1999).
[12] R. B. Li, Z. W. Yao, K. Wang, S. B. Lu, L. Cao, J. Wang, and M. S. Zhan, Phys. Rev. A **94**, 033613 (2016).

[13] E. Arimondo, M. Inguscio, and P. Violino, Rev. Mod. Phys. **49**, 31 (1977).
[14] H. Marion, F. P. Dos Santos, M. Abgrall, S. Zhang, Y. Sortais, S. Bize, I. Maksimovic, D. Calonico, J. Grunert, C. Mandache, P. Lemonde, G. Santarelli, P. Laurent, A. Clairon, and C. Salomon, Phys. Rev. Lett. **90**, 150801 (2003).
[15] J. C. Berengut, V. V. Flambaum, and E. M. Kava, Phys. Rev. A **84**, 042510 (2011).
[16] S. G. Karshenboim, Can. J. Phys. **78**, 639 (2000).
[17] K. Gibble and B. J. Verhaar, Phys. Rev. A **52**, 3370 (1995).
[18] S. J. J. M. F. Kokkelmans, B. J. Verhaar, K. Gibble, and D. J. Heinzen, Phys. Rev. A **56**, R4389 (1997).
[19] G. Petit and Z. Jiang, Metrologia **45**, 35 (2008).
[20] T. P. Heavner, S. R. Jefferts, E. A. Donley, J. H. Shirley, and T. E. Parker, Metrologia **42**, 411 (2005).
[21] V. Gerginov, N. Nemitz, S. Weyers, R. Schroder, D. Griebsch, and R. Wynands, Metrologia **47**, 65 (2010).
[22] F. Fang, M. S. Li, P. W. Lin, W. L. Chen, N. F. Liu, Y. G. Lin, P. Wang, K. Liu, R. Suo, and T. C. Li, Metrologia **52**, 454 (2015).
[23] G. Breit and I. I. Rabi, Phys. Rev. **38**, 2082 (1931).
[24] J. W. Farley and W. H. Wing, Phys. Rev. A **23**, 2397 (1981).
[25] W. M. Itano, L. L. Lewis, and D. J. Wineland, Phys. Rev. A **25**, 1233 (1982).
[26] T. Lee, T. P. Das, and R. M. Sternheimer, Phys. Rev. A **11**, 1784 (1975).
[27] B. Bederson and V. Jaccarino, Phys. Rev. **87**, 228 (1952).
[28] N. Braslau, G. O. Brink, and J. M. Khan, Phys. Rev. **123**, 1801 (1961).
[29] S. Penselin, G. Winkler, T. Moran, and V. W. Cohen, Phys. Rev. **127**, 524 (1962).
[30] J. Vanier, S. J. Simard, and J. S. Soulanger, Phys. Rev. A **9**, 1031 (1974).

Correction: The previously published Figure 7 contained an error in the axis label and has been replaced.